processes

MDPI

Article

RadicalRetro: A Deep Learning-Based Retrosynthesis Model for Radical Reactions

Jiangcheng Xu [1,2,*], Jun Dong [1,2], Kui Du [3], Wenwen Liu [1,2], Jiehai Peng [4] and Wenbo Yu [1,2,*]

[1] Hangzhou Vocational & Technical College, Hangzhou 310014, China; zd_dongjun@zju.edu.cn (J.D.); 19032573770@163.com (W.L.)
[2] Hangzhou Engineering Research Center for Key Technology Improvement and Application of Novel Bio-Based Materials, Hangzhou 310014, China
[3] School of Chemistry and Chemical Engineering, Shaoxing University, Shaoxing 312000, China; dkui@usx.edu.cn
[4] Zhejiang Medicine Co., Ltd., Hangzhou 310014, China; 13819766002@163.com
* Correspondence: 2013010024@hzvtc.edu.cn (J.X.); 2007010003@hzvtc.edu.cn (W.Y.)

Abstract: With the rapid development of radical initiation technologies such as photocatalysis and electrocatalysis, radical reactions have become an increasingly attractive approach for constructing target molecules. However, designing efficient synthetic routes using radical reactions remains a significant challenge due to the inherent complexity and instability of radical intermediates. While computer-aided synthesis planning (CASP) has advanced retrosynthetic analysis for polar reactions, radical reactions have been largely overlooked in AI-driven approaches. In this study, we introduce RadicalRetro, the first deep learning-based retrosynthesis model specifically tailored for radical reactions. Our work is distinguished by three key contributions: (1) RadicalDB: A novel, manually curated database of 21.6 K radical reactions, focusing on high-impact literature and mechanistic clarity, addressing the critical gap in dedicated radical reaction datasets. (2) Model Innovation: By pretraining Chemformer on ZINC-15 and USPTO datasets followed by fine-tuning with RadicalDB, RadicalRetro achieves a Top-1 accuracy of 69.3% in radical retrosynthesis, surpassing the state-of-the-art models LocalRetro and Mol-Transformer by 23.0% and 25.4%, respectively. (3) Interpretability and Practical Utility: Attention weight analysis and case studies demonstrate that RadicalRetro effectively captures radical reaction patterns (e.g., cascade cyclizations and photocatalytic steps) and proposes synthetically viable routes, such as streamlined pathways for Tamoxifen precursors and glycoside derivatives. RadicalRetro's performance highlights its potential to transform radical-based synthetic planning, offering chemists a robust tool to leverage the unique advantages of radical chemistry in drug synthesis.

Keywords: radical reactions; retrosynthesis; deep learning; drug synthesis

check for updates

Academic Editors: Chi-Min Shu and Vincenzo Russo

Received: 17 April 2025
Revised: 27 May 2025
Accepted: 3 June 2025
Published: 5 June 2025

Citation: Xu, J.; Dong, J.; Du, K.; Liu, W.; Peng, J.; Yu, W. RadicalRetro: A Deep Learning-Based Retrosynthesis Model for Radical Reactions. *Processes* **2025**, *13*, 1792. https://doi.org/10.3390/pr13061792

Copyright: © 2025 by the authors. Licensee MDPI, Basel, Switzerland. This article is an open access article distributed under the terms and conditions of the Creative Commons Attribution (CC BY) license (https://creativecommons.org/licenses/by/4.0/).

1. Introduction

Since E. J. Corey [1] first introduced the concept of retrosynthesis, polar disconnections (two-electron reactions) have been widely adopted due to their intuitive nature and ease of understanding. Classical cross-coupling reactions, such as the Suzuki [2], Negishi [3], and Heck [4] reactions, as well as polar addition reactions like the Aldol reaction [5], Michael addition [6,7], and the Grignard reaction [8], are mainstream methods for constructing pharmaceutical molecules. In contrast, the intrinsic instability and low controllability of radicals have historically hindered the development of radical chemistry (single-electron reactions) [9,10]. Nonetheless, recent advancements, particularly in chemical oxidation [11,12],

photocatalysis [13,14], and electrocatalysis [15,16], have led to exciting progress. Compared to two-electron processes, radical reactions exhibit unique advantages, including sequential bond formation (e.g., cascade cyclization), high stereoselectivity and regioselectivity, and excellent functional group tolerance [17–19]. These features make radical chemistry an increasingly powerful tool in modern synthesis, playing a crucial role in the development of drugs for cancer, viral infections, malaria, hyperlipidemia, and depression [17].

This raises a pivotal question: Can we design synthetic routes for known drugs or candidate compounds by harnessing the unique characteristics of radical reactions? Furthermore, how can reactants be tailored to effectively leverage radical chemistry effectively for drug development? Addressing these challenges requires not only deep theoretical insight but also extensive laboratory experience and iterative experimentation to ensure reliable and practical outcomes. With the rapid development of pharmaceutical big data, AI-based retrosynthesis models [20–22] targeting specific reaction types, such as biocatalysis [23,24] and carbohydrate chemistry [25], are continually being developed. However, to the best of our knowledge, there has yet to be a deep learning-based retrosynthesis AI model specifically designed for radical reactions. A likely reason for this is the absence of dedicated databases for radical transformations. Training AI models using general chemical reaction databases (such as USPTO [26], Reaxys [27], ChEMBL [28], and SciFinder [29]) may result in the unique features of radical reactions being overlooked.

This study collected high-impact studies in the literature on radical reactions, with a particular focus on radical-mediated coupling and cyclization reactions for drug molecule construction. By analyzing reaction mechanisms, we built the first dedicated database for radical reactions, termed RadicalDB (Radical Reaction Database). Following model selection and optimization of training strategies with deep learning, we developed a retrosynthesis model specifically designed to capture the unique features of radical chemistry, which we named RadicalRetro. Test results demonstrated that RadicalRetro effectively recognizes radical reaction features and utilizes radical-involved coupling and cyclization methods to design synthetic routes for drugs. Attention weight analysis showed that RadicalRetro exhibits strong interpretability in single-step retrosynthesis design for drug molecules. By developing this AI model for retrosynthetic analysis of radical reactions, this study advances the application of radical reactions in drug synthesis.

2. Results and Discussion

2.1. Construction and Analysis of the Radical Reaction Database (RadicalDB)

2.1.1. Data Collection Strategy for RadicalDB

Building on our research group's expertise in radical chemistry [30] and AI-assisted drug synthesis [31], this study manually curated hundreds of high-impact journal articles, gathering a total of 21.6 K radical reactions. Special attention was given to the mechanisms of these reactions during the literature review to avoid missing any reactants. The chemical reactions in both data sources are represented using SMILES notation [32], with reactants separated by a "." and reactants and products separated by ">>". Each reaction entry is accompanied by its literature source. RadicalDB is an open database.

2.1.2. Composition and Distribution of RadicalDB Data

Multi-component radical reactions (green) account for 47.3% of all entries in RadicalDB, making them the dominant reaction type in the database. These reactions are known for their high atom economy and operational simplicity [33,34], highlighting the value of RadicalDB through their significant proportion. Figure 1a shows that both multi-component radical reactions (green) and bi-component reactions (pink) exhibit a normal distribution of product molecular weights. The overall molecular weight distribution of products

in the dataset (Figure 1b) ranges from 80 to 965 and also follows a normal distribution, indicating that the data in RadicalDB is homogeneous. This suggests that the database minimizes the overrepresentation of structurally similar radical reactions, maintaining a diverse dataset [35].

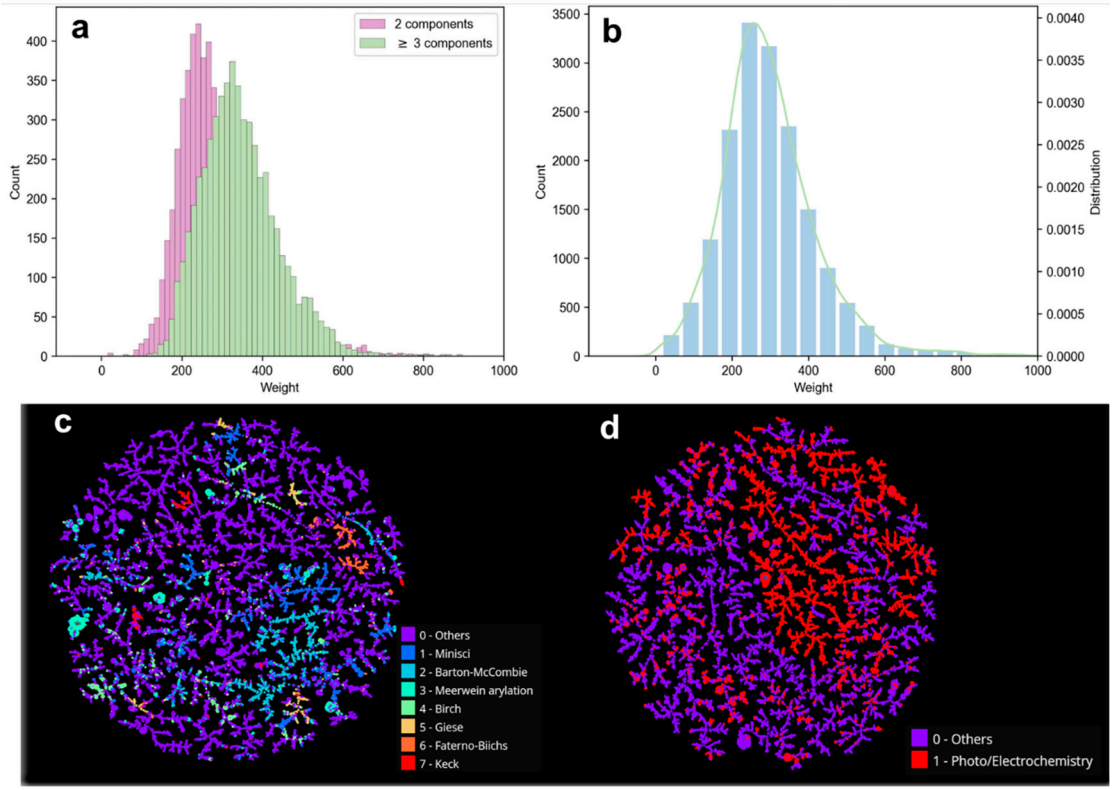


Figure 1. Statistical overview and distribution of data in RadicalDB. (**a**) Multi-component radical reactions represent 47.3% of the database, and the molecular weights of their products across different component types follows a normal distribution. (**b**) The overall molecular weight distribution of radical reaction products in RadicalDB also exhibits a normal distribution. (**c**) RadicalDB includes classic named reactions, each well-clustered according to its reaction type. (**d**) Photocatalytic and electrocatalytic radical reactions constitute 31.6% of RadicalDB. However, some photo-/electrocatalytic reactions (indicated by the red dots in the lower-left corner) show less distinct clustering among radical reactions.

To further analyze the dataset, we utilized T-map [36], a tree-based unsupervised learning algorithm, to visualize RadicalDB. Overall, the data does not exhibit excessive clustering, providing additional evidence that RadicalDB has not over-collected similar types of radical reactions. As shown in Figure 1c, RadicalDB contains classic named radical reactions such as Barton–McCombie [37], Birch [38], Giese [39], Keck [40], and Minisci [41] reactions. These named reactions are well-classified in the chemical space, forming distinct clusters, demonstrating that T-map effectively distinguishes the characteristic types of these reactions.

We also analyzed the rapidly growing subset of photocatalytic and electrocatalytic radical reactions in recent years, labeling them separately from other radical types. From Figure 1d, it is evident that photocatalytic/electrocatalytic reactions (red) account for a significant portion of RadicalDB, accounting for 31.6% of the dataset. Unlike the typical clustering of named reactions, the red points in the lower-left corner of Figure 1c are evenly distributed in space, blending smoothly with general radical reactions (purple). This indicates that photocatalytic/electrocatalytic radical reactions do not exhibit distinct characteristic differences from other general radical reactions. In other words, there is

a high potential for general radical reactions to be optimized through photocatalytic or electrocatalytic synthetic methods.

2.2. Training and Testing of the Radical Reaction Retrosynthesis Prediction Model (RadicalRetro)

To select a deep learning model suitable for the task of radical reaction retrosynthesis, we chose three models that have achieved state-of-the-art (SOTA) performance in single-step retrosynthesis on the USPTO-50K dataset. These models include the graph neural network-based LocalRetro [42], the natural language processing-based Mol-Transformer [43], and Chemformer [44]. Among them, LocalRetro is a template-based deep learning model, while Mol-Transformer and Chemformer are template-free deep learning models.

(1) Training Strategy for Mol-Transformer. Mol-Transformer typically employs transfer learning [25,45] to enhance its performance. In this study, a multi-task strategy [46] was used by combining the USPTO dataset with the target dataset (RadicalDB) for training, allowing the Transformer model to learn both the USPTO dataset (containing 1 M reactions) and the chemical reaction features of RadicalDB. The ratio for mixed sampling was set at 9:1 (USPTO/RadicalDB).

(2) Training Strategy for LocalRetro. First, DGL-LifeSci (https://github.com/awslabs/dgl-lifesci (accessed on 17 April 2025.)) was used to initialize the features of atoms and bonds, with the molecules in RadicalDB represented as graphs, where vertices denote atoms and edges denote bonds. The message passing neural network (MPNN) [47] was applied to update the features of each atom, considering its neighboring atoms and bonds. Local reaction templates were then extracted by comparing the atomic mapping differences between products and reactants. This process resulted in the identification of 2877 radical reaction retrosynthesis templates, including 2227 bond-changing templates and 1342 atom-changing templates. LocalRetro applies a global reaction attention mechanism (GRA) [42] to account for non-local effects in chemical reactions, using template classifiers to score the templates. During retrosynthesis analysis, the model predicts a set of local reaction templates for each chemical center, and these predicted templates are ranked by score to derive the final reactants.

(3) Training Strategy for Chemformer. First, the ZINC-15 dataset [48] (containing 100 million molecules) was used for molecular pretraining. The pretraining process involved masking molecular SMILES codes, primarily through a span-masking algorithm, where short sequences within the SMILES were randomly replaced with a single "<MASK>" token to help the model better understand the combination patterns of atoms and bonds (Figure 2, ①). Next, reaction pretraining was conducted using the USPTO dataset [26] (containing 1 M reactions), allowing the model to learn chemical reaction patterns and features (Figure 2, ②). Finally, fine-tuning was performed on the RadicalDB to help the model grasp the specifics and patterns of radical reactions (Figure 2, ③). The resulting retrosynthesis Chemformer model, after molecular pretraining, reaction pretraining, and RadicalDB fine-tuning, was named RadicalRetro.

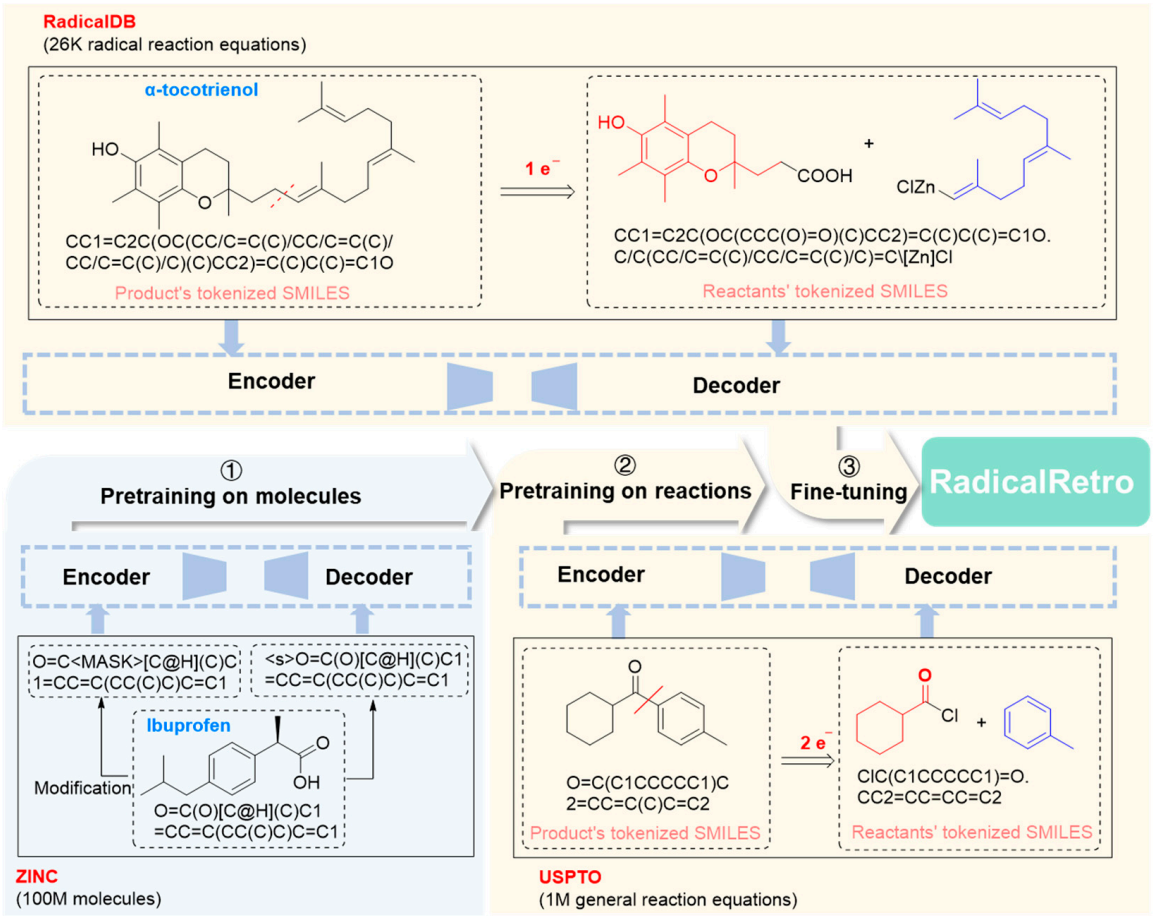


Figure 2. Training strategy diagram of RadicalRetro. The Chemformer model, initially pretrained on 100 million molecules and 1 million reactions, was fine-tuned using RadicalDB to develop the retrosynthesis model, RadicalRetro, specifically tailored for radical reactions.

3. Test Results and Analysis

This section analyzes the test results of the radical reaction retrosynthesis model. To minimize testing errors, 5-fold cross-validation was used to evaluate the results. For each cross-validation experiment, RadicalDB was split into a ratio of 8:1:1 for training, validation, and testing, respectively. The model's performance in predicting radical reactions was compared using Top-K accuracy (K = 1, 3, 5, 10) as the evaluation metric.

The performance of the three models in the task of retrosynthesis prediction for radical reactions is shown in Figure 3. As illustrated in Figure 3a, RadicalRetro, trained using the Chemformer model, achieved the best performance in this task, with an average Top-1 accuracy of 69.31%. The average Top-K (K = 3, 5, 10) accuracies were 76.11%, 78.24%, and 80.07%, respectively, demonstrating that the training strategy of RadicalRetro is scientifically sound and effective. The second-best-performing model was LocalRetro, with an average Top-1 accuracy of 46.35% and average Top-K (K = 3, 5, 10) accuracies of 55.63%, 59.21%, and 61.42%. MolTransformer's performance was slightly lower than that of LocalRetro, achieving a Top-1 accuracy of 43.91% and average Top-K (K = 3, 5, 10) accuracies of 55.89%, 60.36%, and 63.54%.

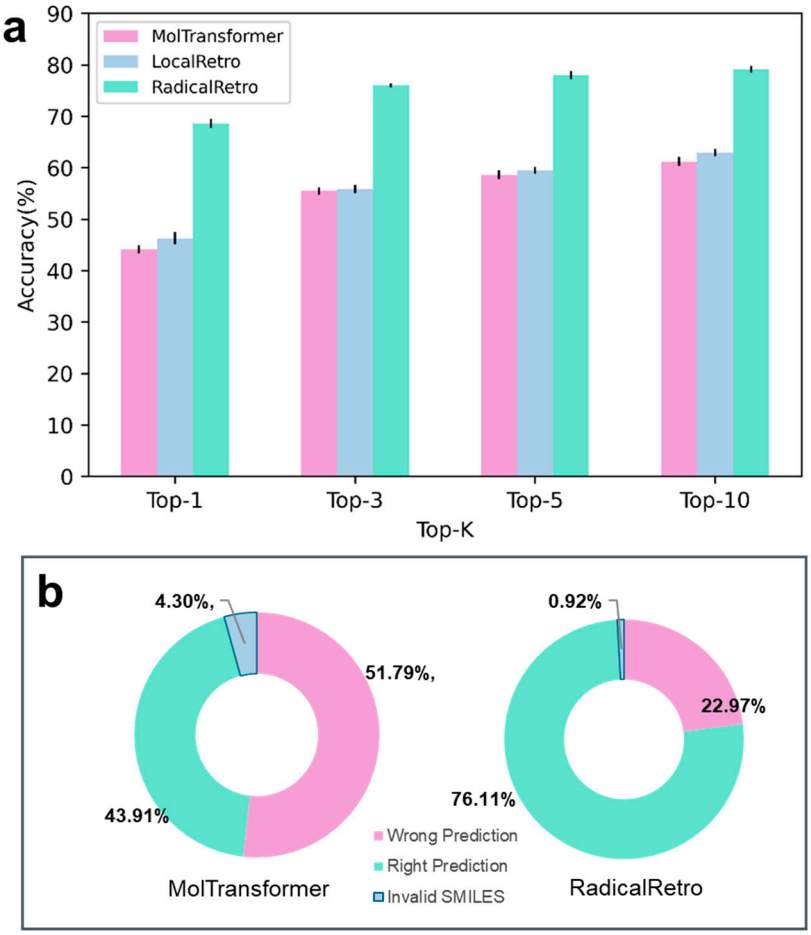


Figure 3. Comparison of the prediction results of the three models. (**a**) RadicalRetro, based on the Chemformer model, achieved the highest prediction accuracy. (**b**) RadicalRetro outperformed MolTransformer in avoiding invalid SMILES predictions.

It is worth noting that in the single-step retrosynthesis task on the USPTO-50K dataset, the prediction performance of Chemformer, LocalRetro, and MolTransformer was relatively similar, with Top-1 accuracies of 54.3% [44], 53.4% [42], and 51.4% [49], respectively. The difference in prediction performance in this task may be attributed to the fact that radical reactions represent a newer type of reaction, especially driven by the rapid advancement of photocatalytic and electrocatalytic technologies over the past decade [34]. The USPTO dataset contains relatively few radical reactions [35], which likely limited MolTransformer's ability to fully extract the characteristic features of radical reactions during training. This hypothesis is further supported by the proportion of invalid SMILES generated by MolTransformer and RadicalRetro (Figure 3b). Additionally, the relatively small number of reactions in RadicalDB (26,000 reactions) may not have been sufficient for LocalRetro to fully extract relevant reaction templates, contributing to the larger performance gap between LocalRetro and RadicalRetro.

RadicalRetro, on the other hand, benefited from molecular pretraining, which enabled the model to learn atomic composition features, and from reaction pretraining, which helped it capture bond change patterns. Moreover, RadicalDB's reaction data was collected using methods that explored reaction mechanisms, ensuring consistent data quality, thereby enabling RadicalRetro to achieve higher retrosynthesis prediction accuracy for radical reactions compared to USPTO-50K.

Analysis of RadicalRetro's Retrosynthesis Prediction Results for Different Types of Radical Reactions.

To investigate the predictive performance of RadicalRetro across different reaction types, this study analyzed the first set of data from the 5-fold cross-validation experiments, and the results are shown in Figure 4. From the perspective of radical initiation methods (Figure 4a), the model achieved a Top-1 accuracy of 71.22% for photocatalytic and electrocatalytic radical reactions compared to 60.96% for other radical reaction types.

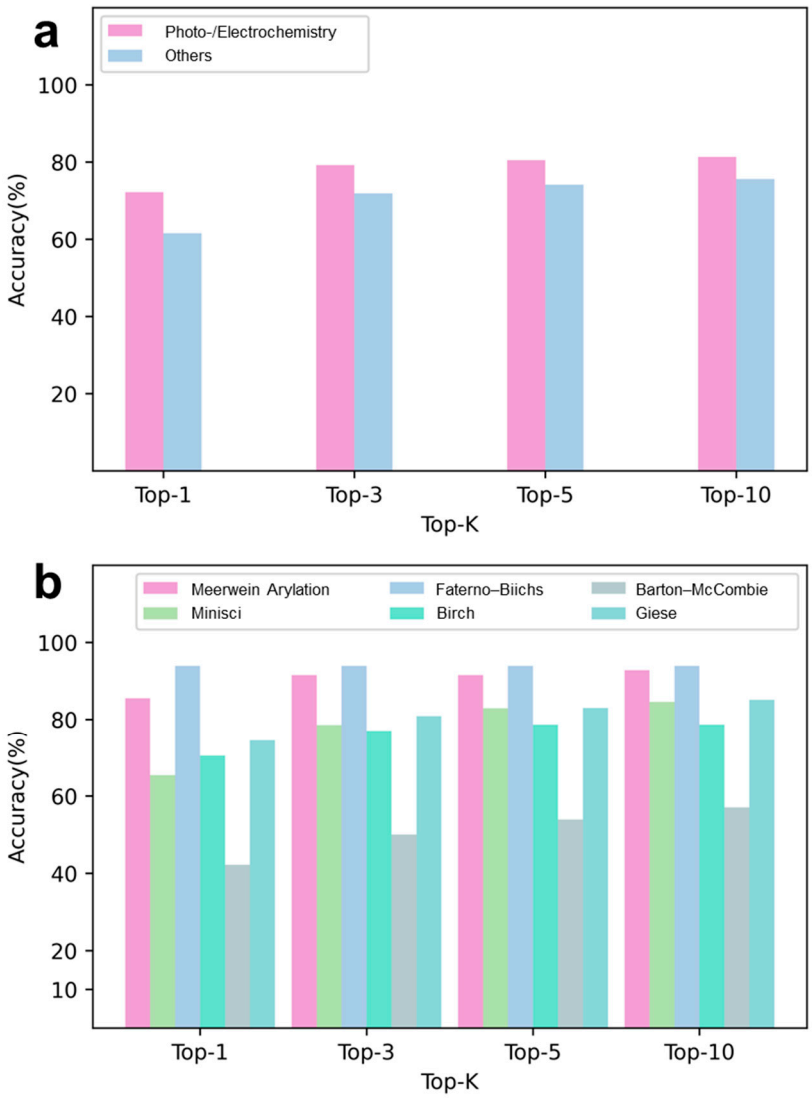


Figure 4. Comparison of RetroSynthesis accuracy of RadicalRetro across different types of radical reactions. (**a**) From the perspective of radical initiation, the retrosynthesis accuracy for photocatalytic and electrocatalytic radical reactions is slightly higher than that for other types of radical reactions. (**b**) In terms of named reactions, the Faterno–Biichs reaction and the Meerwein arylation reaction exhibit the highest retrosynthesis prediction accuracy. However, due to the abundance of C-H bonds in molecules, the model struggled to determine which hydrogen atom in the precursor was originally part of a hydroxyl group. As a result, the Barton–McCombie deoxygenation radical reaction shows the lowest retrosynthesis prediction accuracy.

This performance difference may be attributed to the composition of the RadicalDB dataset. Although the number of photocatalytic and electrocatalytic radical reactions (11,900) is slightly lower than that of other radical reactions (14,100), these reactions have undergone exponential growth in recent years and have received more concentrated research attention. As a result, the model likely found it easier to learn their reaction patterns. This hypothesis is further supported by the distribution characteristics of photocatalytic and electrocatalytic reactions in RadicalDB, as shown in Figure 1d.

From the perspective of named radical reactions, RadicalRetro achieved the highest retrosynthesis prediction accuracies for the Faterno–Biichs and Meerwein arylation reactions, with Top-1 accuracies of 92.31% and 84.12%, respectively. The prediction accuracies for Birch, Giese, and Minisci reactions were close to or exceeded the overall average. However, the retrosynthesis prediction accuracy for the Barton–McCombie deoxygenation radical reaction was the lowest, with a Top-1 accuracy of only 41.13%, significantly below the average accuracy of RadicalRetro. This lower performance may stem from the inherent nature of the reaction: in the Barton–McCombie reaction, a hydroxyl group in an organic compound is replaced by a hydrogen atom [43]. Since drug molecules typically have an abundance of C-H bonds, the model struggles to determine which hydrogen atom in the precursor was originally part of a hydroxyl group. From this perspective, the achieved prediction accuracy for the Barton–McCombie reaction can still be considered relatively ideal.

In summary, RadicalRetro exhibited strong retrosynthesis prediction performance across both different radical initiation methods and named reactions, highlighting the effectiveness of the Transformer model with molecular and reaction pretraining in the domain of chemical synthesis.

Interpretability of RadicalRetro

Good interpretability is essential for building user trust and facilitating the effective management of AI tools. It not only helps users understand the decision-making process of AI but also enhances their confidence in using these systems. Furthermore, clear interpretability is essential for monitoring and adjusting AI applications to ensure they meet the specific needs of a given domain [50].

In the drug synthesis process, radical reactions typically proceed through the following key steps [9]: (1) Radical generation: The reaction begins with the formation of radicals, which can be initiated by various methods, such as photocatalysis [14], electrocatalysis [15], mechanochemistry [51], or the use of specific chemical reagents [52]. (2) Radical addition or abstraction: Radicals undergo addition to unsaturated bonds or abstract atoms (commonly hydrogen) from saturated molecules. (3) Chain propagation: Radical reactions often proceed through a chain mechanism. In the chain propagation step, newly formed radicals continue to react with other molecules, generating more radicals and perpetuating the reaction. (4) Chain termination: When two radicals combine to form a stable molecule, the radical chain is terminated. Therefore, retrosynthetic analysis of radical reactions must consider not only the global and local structures of the target molecule (such as functional group substitutions) but also the generation, propagation, and termination of radicals.

In this section, we explore the interpretability of RadicalRetro by selecting a phenylindene scaffold molecule which has been shown to exhibit various biological activities [53]. Specifically, we analyzed the retrosynthetic prediction of 2-(2-phenyl-1H-ind-1-yl)acetonitrile **1**. RadicalRetro predicted the precursors to be 3-(2-phenylethynylphenyl)acrylonitrile **2** and tributyltin **3** (Figure 5a). The rationale behind this retrosynthetic route has been confirmed by the work of the Alabugin group [54], and the reaction process shown in the figure was computationally validated.

The attention weight heatmap (Figure 5c) and attention entropy distribution (Figure S1a, ESI†) reveal several insights: On a global scale, the predicted precursor structures (on the vertical axis) focused on the overall structure of **1** (on the horizontal axis). When generating tributyltin **3**, which only serves as a radical initiator, the model paid attention to the entire structure of **1**. However, when generating precursor **2**, the model focused on the detailed structure of **1**. Locally, when generating the radical receptor alkene structure "C=C" in **2**, the model paid attention to the chemical environment of the α and β carbons of the electron-withdrawing nitrile group (region **1′**) and the structural information of the

phenyl ring (region **2′**). When generating the radical receptor alkyne structure "C≡C" in **2**, the model focused on the chemical structure surrounding the indene (region **3′**) and the structural information of the unsaturated bonds within the indene scaffold (region **4′**). This global-to-local attention mechanism aligns well with the mechanistic studies conducted by the Alabugin group [54] and reflects the way chemists approach retrosynthetic analysis.

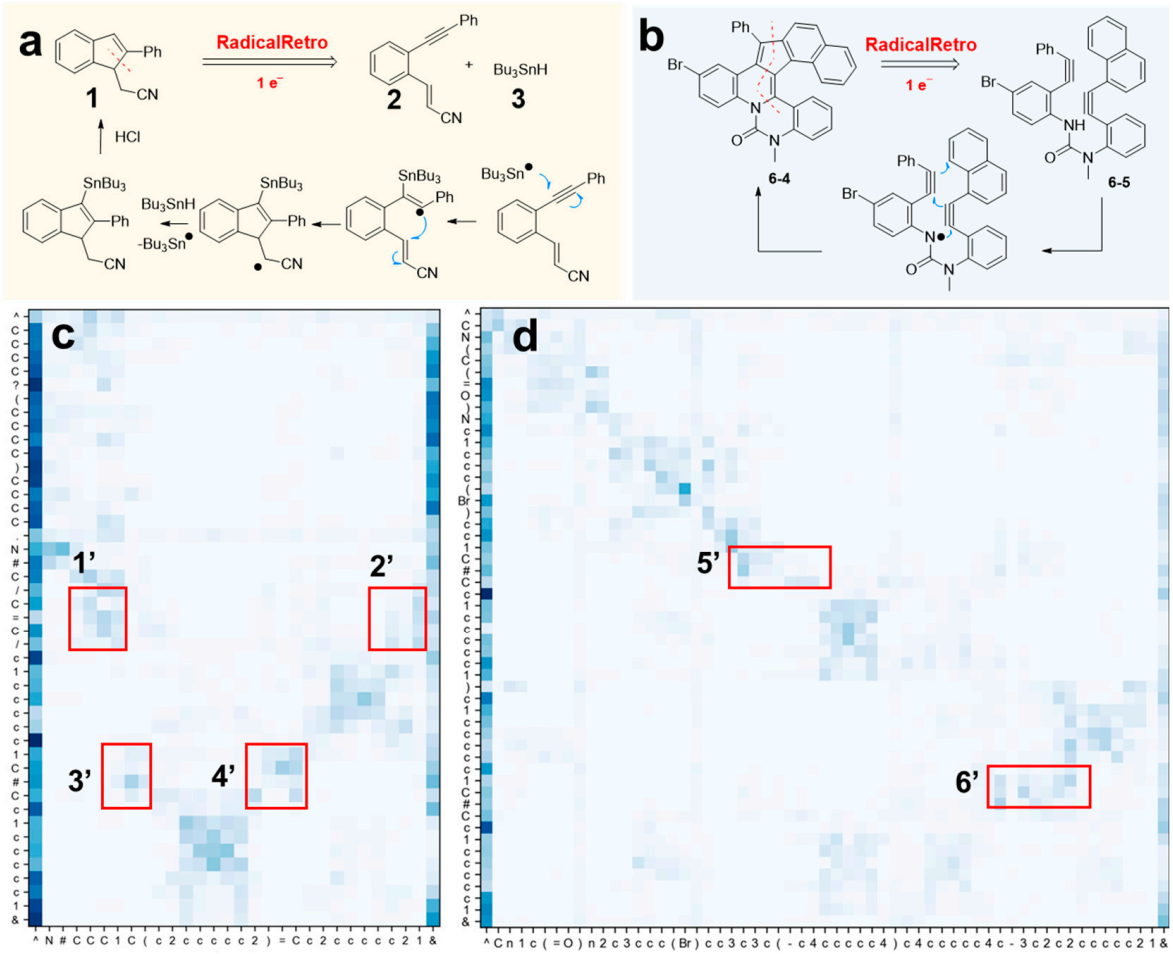


Figure 5. Interpretability of LocalRetro. (**a**,**b**) demonstrate that RadicalRetro successfully identifies the appropriate radical reaction pathways for synthesizing biologically active phenylindane scaffold molecules and nitrogen-containing polycyclic aromatic hydrocarbons, respectively. (**c**,**d**) illustrate that, during the retrosynthesis process for these two compounds, RadicalRetro's attention mechanism, from global to local, aligns closely with how chemists approach retrosynthetic analysis, confirming the interpretability of the model.

This study also selected a fused-ring scaffold molecule as a case for retrosynthetic analysis to explore the interpretability of RadicalRetro. Azapolycyclic aromatic hydrocarbons (PAHs) **4**, due to the electron-donating nitrogen atom, are prone to oxidative decomposition, making their synthesis particularly challenging [55]. When RadicalRetro was used for the retrosynthetic analysis of **4** (Figure 5b), it predicted the precursor to be a diyne **5**, which undergoes a radical cascade cyclization reaction. The validity of this retrosynthetic route was confirmed by the Xu group's work on electrocatalytic synthesis of PAHs [56]. From the attention heatmap of RadicalRetro's retrosynthetic analysis (Figure 5d) and attention entropy distribution (Figure S1b, ESI†), it can be seen that the structure of diyne **5** was generated based on the structure of the PAH. The structural information of the precursor can be correspondingly traced back to **4**. Interestingly, the two alkyne groups "C≡C" formed through the "cleavage" characteristic of radical reactions were generated based on

the structural information of the two aromatic rings in **4** (regions **5′** and **6′**). The attention mechanism analysis aligns with the mechanistic pathway proposed by Takase et al. [55] and mirrors the logical patterns employed by human chemists in retrosynthetic analysis. These cases demonstrate that RadicalRetro shows good interpretability when performing retrosynthetic analysis based on the characteristics of radical reactions. Further examples are shown in Figures S2–S4 (ESI†).

4. Application of RadicalRetro in Synthesis

Retrosynthetic Analysis Using Radical Reaction Characteristics

In this section, we explore whether RadicalRetro effectively learned the principles of radical reactions through specific retrosynthetic analysis cases. In this study, the Chemformer model, trained with molecular and reaction pretraining but without fine-tuning on the RadicalDB dataset, is referred to as GeneralRetro, which serves as the baseline model for RadicalRetro. Several drug intermediates were selected for retrosynthetic analysis using both GeneralRetro and RadicalRetro, and their outputs were systematically compared (Figure 6).

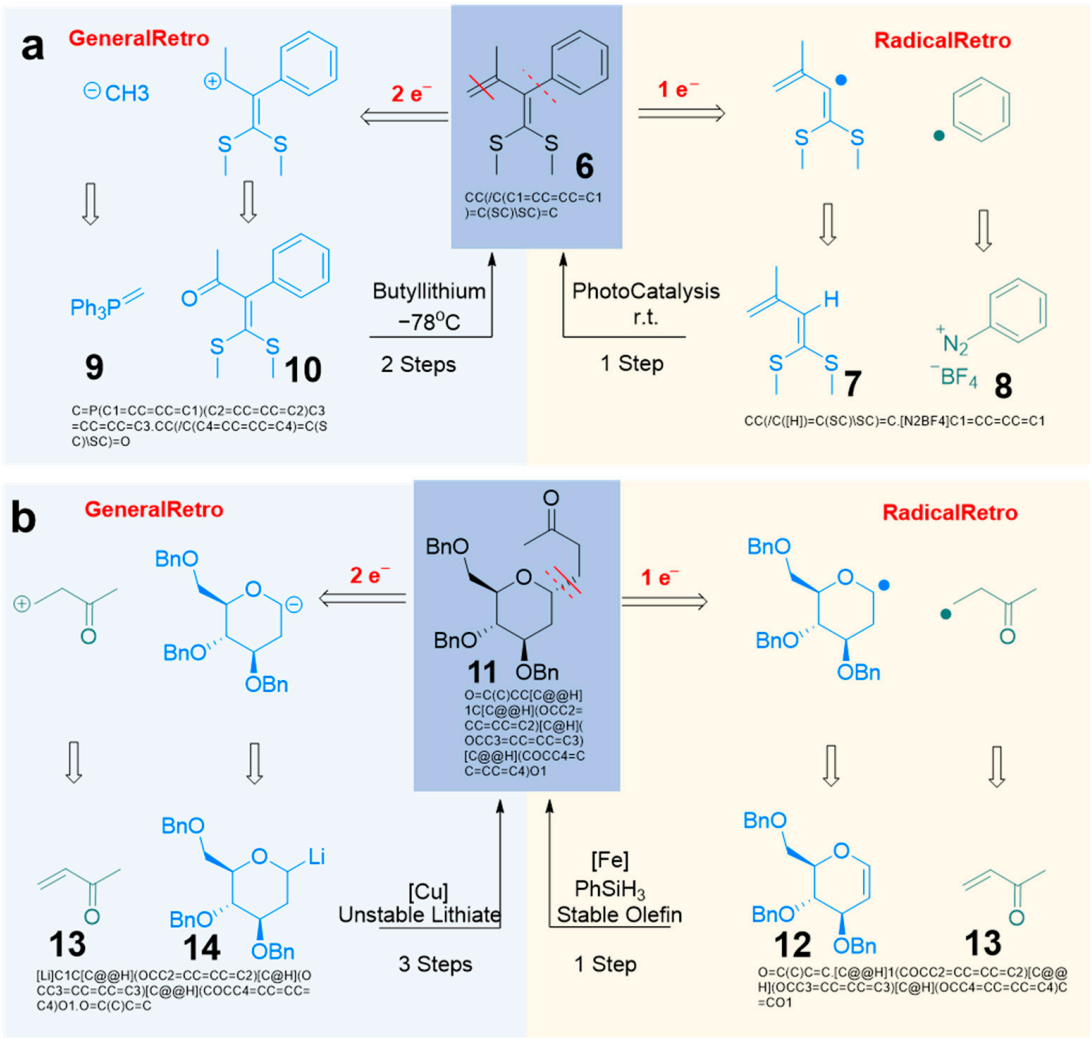


Figure 6. Comparison of the retrosynthesis between RadicalRetro and GeneralRetro. For the Tamoxifen precursor (**a**) and glycoside derivative (**b**): compared to GeneralRetro without fine-tuning on RadicalDB, the synthesis pathways proposed by RadicalRetro demonstrate a better grasp of radical reaction characteristics. This approach shows significant potential in reducing reaction steps and optimizing reaction conditions [9].

Through case analysis, it was found that RadicalRetro can leverage the characteristics of radical reactions to design synthetic routes involving radical-mediated coupling reactions. For example, 1,1-S,S-functionalized tetrasubstituted alkene 6 is the starting material for the estrogen receptor modulator Tamoxifen [57] (Figure 6a). When retrosynthetically analyzing this molecule using the two AI models trained in this study, two different synthetic strategies were provided: GeneralRetro suggested the starting materials for a Wittig reaction, namely, triphenylphosphine 9 and 4,4-bis(methylthio)-3-phenylbut-3-en-2-one 10. This route is one that would commonly come to mind for chemists, and it has been used in recent synthesis efforts by Zhang's group and Monfette's group [57,58]. In contrast, RadicalRetro proposed a strategy involving radical coupling, with the predicted precursors being (3-methylbut-1,3-diene-1,1-diyl)bis(methylthio) 7 and phenyl diazonium salt 8. Upon reviewing the literature, we found that this route's rationale was supported by recent photocatalytic synthesis work by Yu's group [59]. Comparing the two retrosynthetic strategies, the strategy proposed by GeneralRetro involves the use of unstable ylides, requiring low temperatures (−78 °C) and strong bases (e.g., tert-butyllithium) across two steps [57]. In contrast, the photocatalytic coupling strategy suggested by RadicalRetro only requires a small amount of photosensitizer and can proceed under mild conditions, such as room temperature and light exposure, making the reaction conditions milder and the process simpler [59].

Another case is the synthesis of glycoside derivative 11 (Figure 6b). Glycoside derivatives have been shown to possess biological activity, including anticancer and anti-Alzheimer's effects [60]. When both AI models were used to analyze the retrosynthesis of glycoside derivative 11, they proposed two different synthetic strategies: GeneralRetro suggested a Michael addition route, with the precursors being organolithium compound 14 and the Michael acceptor but-3-en-2-one 13, consistent with the strategy employed by Suginome's group [61]. In contrast, RadicalRetro proposed a hydrogen atom transfer-initiated radical coupling retrosynthesis, with the precursors being the more stable alkene derivative 12 and radical acceptor 13. This approach aligns with the synthesis method reported by Baran's group [62]. Of the two retrosynthesis routes, RadicalRetro's strategy avoids the use of unstable precursors like organolithium compounds and reduces the number of steps by two compared to GeneralRetro, offering a more efficient radical-mediated coupling strategy.

These retrosynthesis cases demonstrate that, compared to GeneralRetro, which was not fine-tuned on RadicalDB, RadicalRetro is better able to utilize the characteristics of radical reactions and propose radical-based synthetic strategies in drug retrosynthesis predictions. This highlights the significant impact that fine-tuning with RadicalDB had on the performance of the deep learning model.

5. Conclusions

Deep learning models have been applied to retrosynthetic analysis across various types of reactions, but the analysis of single-electron transfer (SET) retrosynthesis has not received sufficient attention or in-depth study. This study presents a data-driven model, RadicalRetro, designed to leverage the characteristics of radical reactions for retrosynthetic analysis of drug molecules. After model selection, the natural language processing-based Chemformer was found to be suitable for the task of predicting radical reaction retrosynthesis in drug synthesis. RadicalRetro learned atomic arrangement features through molecular pretraining, organic synthesis reaction features through reaction pretraining, and radical reaction characteristics through fine-tuning. It effectively utilizes features such as radical-mediated coupling and cyclization reactions to design synthetic routes, achieving an average Top-1 accuracy of 69.31% and a Top-10 accuracy of 80.07% in radical reaction retrosynthesis prediction. RadicalRetro demonstrated consistent performance across different

types of radical reaction retrosynthesis tasks. Attention weight analysis of the model indicates that the output of products considers both the global structural information and local functional group details of the target molecule, showcasing the model's interpretability.

While these results are promising, several important considerations emerge. First, the model's predictive capability is necessarily constrained by RadicalDB's current composition, which emphasizes well-established, high-yielding transformations at the potential expense of emerging radical methodologies. Second, like all retrosynthetic prediction tools, RadicalRetro identifies plausible disconnections without explicit consideration of kinetic or thermodynamic feasibility. Looking ahead, we envision multiple research directions, including database expansion to incorporate underrepresented radical systems (metalloradical species and electrochemical pathways), the development of integrated condition prediction modules, and the creation of hybrid human–AI interfaces that combine computational predictions with expert synthetic intuition. Most significantly, this work establishes a foundation for systematic exploration of radical chemistry in drug synthesis through AI assistance, potentially unlocking new synthetic strategies that complement traditional polar disconnections.

6. Methods

6.1. Data Curation

RadicalDB was constructed through systematic screening of 3245 studies (2010–2023). Inclusion criteria required experimentally verified reactions, a $\geq$50% reported yield, and clearly characterized products. Reactions were annotated using RDKit (v2022.09) with SMILES standardization.

6.2. Deep Learning Models and Parameters

6.2.1. Chemformer

Chemformer is a deep learning model based on BART (Bidirectional and Auto-Regressive Transformer), commonly used for generative tasks such as text summarization and machine translation. The main parameter settings for Chemformer in this study were as follows:

```
python -m molbart.fine_tune \;
-dataset uspto_50 \;
-data_path data/radicals/radicals_fold${fold}.pkl \;
-task backward_prediction \;
-n_epochs 100 \;
-lr 0.001 \;
-schedule cycle \;
-batch_size 64 \;
-acc_batches 4 \;
-augmentation_strategy all \;
-aug_prob 0.5.
```

6.2.2. Mol-Transformer

Mol-Transformer is a natural language processing model specifically designed for chemical reactions and is based on the Transformer architecture. This study utilized the multi-task learning method provided by OpenNMT. The mixed sampling ratio for training was set at 9:1 (USPTO/RadicalDB). Other parameters were consistent with the research by Probst's group, with the main parameter settings as follows:

```
onmt_train -data ${DATASET} \;
-save_model ${OUTDIR} \;
```

-data_ids uspto transfer --data_weights 9 1 \;
-seed 42 -gpu_ranks 0 \;
-train_steps 50000 -param_init 0 \;
-param_init_glorot -max_generator_batches 32 \;
-batch_size 4096 -batch_type tokens \;
-normalization tokens -max_grad_norm 0 -accum_count 4 \;
-optim adam -adam_beta1 0.9 -adam_beta2 0.998 -decay_method noam \;
-warmup_steps 800 -learning_rate 2 -label_smoothing 0.0 \;
-layers 2 -rnn_size 384 -word_vec_size 384 \;
-encoder_type transformer -decoder_type transformer \;
-dropout 0.1 -position_encoding -share_embeddings \;
-global_attention general -global_attention_function softmax \;
-self_attn_type scaled-dot -heads 4 -transformer_ff 1024 \;
-tensorboard --tensorboard_log_dir ${LOGDIR}.

6.2.3. LocalRetro

LocalRetro is a template-based deep learning model that achieved 53.4% accuracy on the single-step retrosynthesis task in the USPTO-50K dataset and was once a state-of-the-art (SOTA) model in this field. The main parameter settings were as follows:

python Train.py --gpu cuda:0 --dataset RadicalDB;
-config default_config.json;
-batch-size 16 \;
-num-epochs 50 \;
-patience 5 -max-clip 20 -learning-rate 1e-4 \;
-weight-decay 1e-6 -schedule_step 10 -num-workers 0 \;
-print-every 20.

6.3. Training Strategy

The Chemformer architecture was implemented using the HuggingFace Transformers library (v4.28.1). Pretraining on ZINC-15 employed masked language modeling with 15% token masking probability. Fine-tuning used mixed-precision training (FP16) with gradient clipping (max norm = 1.0). Hyperparameters were optimized via Bayesian search over 200 trials, evaluating validation set Top-1 accuracy. This study employed a multi-task transfer learning approach, using a convex weighting scheme for the USPTO and fine-tuning datasets, with weights of 9 and 1, respectively. This approach was based on the method used by Pesciullesi's group in their study on predicting glycosylation reactions.

The transfer learning data came from the USPTO dataset, originally derived from Lowe's dataset, which was extracted from USPTO patent data. The dataset was preprocessed to remove reagents, solvents, temperatures, and other reaction conditions, and then filtered to eliminate duplicate, incorrect, or incomplete reactions. This dataset contains 1 million reaction records.

6.4. Testing Method

Cross-validation is a widely used machine learning evaluation technique that divides a dataset into mutually exclusive subsets for training and validation, allowing for a comprehensive assessment of a model's performance and generalization ability. This method effectively addresses overfitting and underfitting, providing a thorough understanding of the model's actual performance.

In this study, all models were constructed and evaluated using 5-fold cross-validation, ensuring the robustness of the results. During the 5-fold cross-validation, the study also balanced the different categories of radical reactions by adopting a stratified sampling strategy.

Each category, including photocatalytic/electrocatalytic synthesis reactions and named radical reactions, was randomly sampled. This approach ensured that the models were exposed to various types of radical reactions, thereby enhancing their prediction capabilities.

6.5. Reproducibility

All experiments were run on Ubuntu 20.04 LTS with CUDA 11.7. Random seeds were fixed (42 for data splits, 2023 for model initialization) using PyTorch's deterministic algorithms. Complete environment specifications are provided in the requirements.txt file in our GitHub repository (https://github.com/MolAstra/RadicalRetro (accessed on 17 April 2025)), including dependency versions.

Supplementary Materials: The following supporting information can be downloaded at https://www.mdpi.com/article/10.3390/pr13061792/s1, Figure S1: Attention Entropy Maps for Retrosynthetic Analysis of (a) 2-(2-phenyl-1H-indol-1-yl)acetonitrile and (b) Azapolycyclic Aromatic Hydrocarbons (PAHs).; Figure S2–S4: Cases Study of the RadicalRetro Retrosynthesis Attention Mechanism.

Author Contributions: J.X. designed the research project; J.D., J.P., W.L. and K.D. collected the literature and established RadicalDB; J.X. designed and trained the models; J.X. and W.Y. analyzed the data and wrote the manuscript. All authors discussed the results and approved the manuscript. All authors have read and agreed to the published version of the manuscript.

Funding: This research was supported by the General Research Project of the Zhejiang Provincial Department of Education No. Y202456962 and the Zhejiang Provincial Research Project on Chinese Vocational Education No. ZJCV2024B31.

Data Availability Statement: The RadicalDB and supplementary datasets used in this study and The source code of RadicalRetro and associated data preparation python scripts are available at https://github.com/MolAstra/RadicalRetro (accessed on 17 April 2025).

Conflicts of Interest: Author Jiehai Peng was employed by the company Zhejiang Medicine Co., Ltd. The remaining authors declare that the research was conducted in the absence of any commercial or financial relationships that could be construed as a potential conflict of interest.

References

1. Corey, E.J. Robert Robinson Lecture. Retrosynthetic Thinking–Essentials and Examples. *Chem. Soc. Rev.* **1988**, *17*, 111–133. [CrossRef]
2. Niwa, T.; Uetake, Y.; Isoda, M.; Takimoto, T.; Nakaoka, M.; Hashizume, D.; Sakurai, H.; Hosoya, T. Lewis Acid-Mediated Suzuki–Miyaura Cross-Coupling Reaction. *Nat. Catal.* **2021**, *4*, 1080–1088. [CrossRef]
3. Zhao, B.; Rogge, T.; Ackermann, L.; Shi, Z. Metal-Catalysed C–Het (F, O, S, N) and C–C Bond Arylation. *Chem. Soc. Rev.* **2021**, *50*, 8903–8953. [CrossRef] [PubMed]
4. Bhoyare, V.W.; Sosa Carrizo, E.D.; Chintawar, C.C.; Gandon, V.; Patil, N.T. Gold-Catalyzed Heck Reaction. *J. Am. Chem. Soc.* **2023**, *145*, 8810–8816. [CrossRef]
5. Yamashita, Y.; Yasukawa, T.; Yoo, W.-J.; Kitanosono, T.; Kobayashi, S. Catalytic Enantioselective Aldol Reactions. *Chem. Soc. Rev.* **2018**, *47*, 4388–4480. [CrossRef]
6. Wang, J.; Young, T.A.; Duarte, F.; Lusby, P.J. Synergistic Noncovalent Catalysis Facilitates Base-Free Michael Addition. *J. Am. Chem. Soc.* **2020**, *142*, 17743–17750. [CrossRef]
7. Földes, T.; Madarász, Á.; Révész, Á.; Dobi, Z.; Varga, S.; Hamza, A.; Nagy, P.R.; Pihko, P.M.; Pápai, I. Stereocontrol in Diphenylprolinol Silyl Ether Catalyzed Michael Additions: Steric Shielding or Curtin–Hammett Scenario? *J. Am. Chem. Soc.* **2017**, *139*, 17052–17063. [CrossRef]
8. Guisán-Ceinos, M.; Martín-Heras, V.; Tortosa, M. Regio- and Stereospecific Copper-Catalyzed Substitution Reaction of Propargylic Ammonium Salts with Aryl Grignard Reagents. *J. Am. Chem. Soc.* **2017**, *139*, 8448–8451. [CrossRef]
9. Smith, J.M.; Harwood, S.J.; Baran, P.S. Radical Retrosynthesis. *Acc. Chem. Res.* **2018**, *51*, 1807–1817. [CrossRef]
10. Petzold, D.; Giedyk, M.; Chatterjee, A.; König, B. A Retrosynthetic Approach for Photocatalysis. *Eur. J. Org. Chem.* **2020**, *2020*, 1193–1244. [CrossRef]
11. Mandal, S.; Bera, T.; Dubey, G.; Saha, J.; Laha, J.K. Uses of $K_2S_2O_8$ in Metal-Catalyzed and Metal-Free Oxidative Transformations. *ACS Catal.* **2018**, *8*, 5085–5144. [CrossRef]

12. Hinz, A.; Bresien, J.; Breher, F.; Schulz, A. Heteroatom-Based Diradical(Oid)s. *Chem. Rev.* **2023**, *123*, 10468–10526. [CrossRef]
13. Pitre, S.P.; Overman, L.E. Strategic Use of Visible-Light Photoredox Catalysis in Natural Product Synthesis. *Chem. Rev.* **2022**, *122*, 1717–1751. [CrossRef]
14. Wang, H.; Tian, Y.-M.; König, B. Energy- and Atom-Efficient Chemical Synthesis with Endergonic Photocatalysis. *Nat. Rev. Chem.* **2022**, *6*, 745–755. [CrossRef]
15. Novaes, L.F.T.; Liu, J.; Shen, Y.; Lu, L.; Meinhardt, J.M.; Lin, S. Electrocatalysis as an Enabling Technology for Organic Synthesis. *Chem. Soc. Rev.* **2021**, *50*, 7941–8002. [CrossRef]
16. Rein, J.; Zacate, S.B.; Mao, K.; Lin, S. A Tutorial on Asymmetric Electrocatalysis. *Chem. Soc. Rev.* **2023**, *52*, 8106–8125. [CrossRef]
17. Gupta, A.; Laha, J.K. Growing Utilization of Radical Chemistry in the Synthesis of Pharmaceuticals. *Chem. Rec.* **2023**, *23*, e202300207. [CrossRef]
18. Fischer, H. The Persistent Radical Effect: A Principle for Selective Radical Reactions and Living Radical Polymerizations. *Chem. Rev.* **2001**, *101*, 3581–3610. [CrossRef]
19. Xu, J.; Zhang, P.; Li, W. Synthesis of BCP Nitriles Enabled by a Metallaphotoredox-Based Multi-Component Reaction. *Chem Catal.* **2023**, *3*, 100618. [CrossRef]
20. Yu, T.; Boob, A.G.; Volk, M.J.; Liu, X.; Cui, H.; Zhao, H. Machine Learning-Enabled Retrobiosynthesis of Molecules. *Nat. Catal.* **2023**, *6*, 137–151. [CrossRef]
21. Zhong, Z.; Song, J.; Feng, Z.; Liu, T.; Jia, L.; Yao, S.; Hou, T.; Song, M. Recent Advances in Deep Learning for Retrosynthesis. *WIREs Comput. Mol. Sci.* **2024**, *14*, e1694. [CrossRef]
22. Han, Y.; Xu, X.; Hsieh, C.-Y.; Ding, K.; Xu, H.; Xu, R.; Hou, T.; Zhang, Q.; Chen, H. Retrosynthesis Prediction with an Iterative String Editing Model. *Nat. Commun.* **2024**, *15*, 6404. [CrossRef] [PubMed]
23. Probst, D.; Manica, M.; Nana Teukam, Y.G.; Castrogiovanni, A.; Paratore, F.; Laino, T. Biocatalysed Synthesis Planning Using Data-Driven Learning. *Nat. Commun.* **2022**, *13*, 964. [CrossRef] [PubMed]
24. Finnigan, W.; Hepworth, L.J.; Flitsch, S.L.; Turner, N.J. RetroBioCat as a Computer-Aided Synthesis Planning Tool for Biocatalytic Reactions and Cascades. *Nat. Catal.* **2021**, *4*, 98–104. [CrossRef]
25. Pesciullesi, G.; Schwaller, P.; Laino, T.; Reymond, J.-L. Transfer Learning Enables the Molecular Transformer to Predict Regio- and Stereoselective Reactions on Carbohydrates. *Nat. Commun.* **2020**, *11*, 4874. [CrossRef]
26. Lowe, D. Chemical Reactions from US Patents (1976–2016). Available online: https://figshare.com/articles/Chemical_reactions_from_US_patents_1976-Sep2016_/5104873 (accessed on 17 April 2025).
27. Radestock, S. Optimising Chemical Information Workflows: Integrating Reaxys—Use Cases and Applications. *J. Cheminform.* **2013**, *5*, P39. [CrossRef]
28. Gaulton, A.; Hersey, A.; Nowotka, M.; Bento, A.P.; Chambers, J.; Mendez, D.; Mutowo, P.; Atkinson, F.; Bellis, L.J.; Cibrián-Uhalte, E.; et al. The ChEMBL Database in 2017. *Nucleic Acids Res.* **2017**, *45*, D945–D954. [CrossRef]
29. Somerville, A.N. SciFinder Scholar (by Chemical Abstracts Service). *J. Chem. Educ.* **1998**, *75*, 959. [CrossRef]
30. Xu, J.; Zhang, Y.; Han, J.; Su, A.; Qiao, H.; Zhang, C.; Tang, J.; Shen, X.; Sun, B.; Yu, W.; et al. Providing Direction for Mechanistic Inferences in Radical Cascade Cyclization Using a Transformer Model. *Org. Chem. Front.* **2022**, *9*, 2498–2508. [CrossRef]
31. Xu, J.; Yu, W.; Luo, Y.; Liu, T.; Su, A. Developing Lead Compounds of eEF2K Inhibitors Using Ligand–Receptor Complex Structures. *Processes* **2024**, *12*, 1540. [CrossRef]
32. Zhong, Z.; Song, J.; Feng, Z.; Liu, T.; Jia, L.; Yao, S.; Wu, M.; Hou, T.; Song, M. Root-Aligned SMILES: A Tight Representation for Chemical Reaction Prediction. *Chem. Sci.* **2022**, *13*, 9023–9034. [CrossRef] [PubMed]
33. Guo, H.-M.; Wang, J.-J.; Xiong, Y.; Wu, X. Visible-Light-Driven Multicomponent Reactions for the Versatile Synthesis of Thioamides by Radical Thiocarbamoylation. *Angew. Chem. Int. Ed.* **2024**, *63*, e202409605. [CrossRef]
34. Coppola, G.A.; Pillitteri, S.; Van der Eycken, E.V.; You, S.-L.; Sharma, U.K. Multicomponent Reactions and Photo/Electrochemistry Join Forces: Atom Economy Meets Energy Efficiency. *Chem. Soc. Rev.* **2022**, *51*, 2313–2382. [CrossRef]
35. de Almeida, A.F.; Moreira, R.; Rodrigues, T. Synthetic Organic Chemistry Driven by Artificial Intelligence. *Nat. Rev. Chem.* **2019**, *3*, 589–604. [CrossRef]
36. Probst, D.; Reymond, J.-L. Visualization of Very Large High-Dimensional Data Sets as Minimum Spanning Trees. *J. Cheminform.* **2020**, *12*, 12. [CrossRef]
37. Mahy, W.; Plucinski, P.; Jover, J.; Frost, C.G. Ruthenium-Catalyzed O- to S-Alkyl Migration: A Pseudoreversible Barton–McCombie Pathway. *Angew. Chem. Int. Ed.* **2015**, *54*, 10944–10948. [CrossRef]
38. Nemirovich, T.; Kostal, V.; Copko, J.; Schewe, H.C.; Boháčová, S.; Martinek, T.; Slanina, T.; Jungwirth, P. Bridging Electrochemistry and Photoelectron Spectroscopy in the Context of Birch Reduction: Detachment Energies and Redox Potentials of Electron, Dielectron, and Benzene Radical Anion in Liquid Ammonia. *J. Am. Chem. Soc.* **2022**, *144*, 22093–22100. [CrossRef]
39. Gant Kanegusuku, A.L.; Roizen, J.L. Recent Advances in Photoredox-Mediated Radical Conjugate Addition Reactions: An Expanding Toolkit for the Giese Reaction. *Angew. Chem. Int. Ed.* **2021**, *60*, 21116–21149. [CrossRef]

40. Smith, M.W.; Snyder, S.A. A Concise Total Synthesis of (+)-Scholarisine A Empowered by a Unique C–H Arylation. *J. Am. Chem. Soc.* **2013**, *135*, 12964–12967. [CrossRef]
41. Gu, Y.-J.; Luo, M.-P.; Yuan, H.; Liu, G.-K.; Wang, S.-G. Photocatalytic Enantioselective Radical Cascade Multicomponent Minisci Reaction of β-Carbolines Using Diazo Compounds as Radical Precursors. *Adv. Sci.* **2024**, *11*, 2402272. [CrossRef]
42. Chen, S.; Jung, Y. Deep Retrosynthetic Reaction Prediction Using Local Reactivity and Global Attention. *JACS Au* **2021**, *1*, 1612–1620. [CrossRef] [PubMed]
43. Schwaller, P.; Laino, T.; Gaudin, T.; Bolgar, P.; Hunter, C.A.; Bekas, C.; Lee, A.A. Molecular Transformer: A Model for Uncertainty-Calibrated Chemical Reaction Prediction. *ACS Cent. Sci.* **2019**, *5*, 1572–1583. [CrossRef] [PubMed]
44. Irwin, R.; Dimitriadis, S.; He, J.; Bjerrum, E.J. Chemformer: A Pre-Trained Transformer for Computational Chemistry. *Mach. Learn. Sci. Technol.* **2022**, *3*, 015022. [CrossRef]
45. Zhang, C.; Zhai, Y.; Gong, Z.; Duan, H.; She, Y.-B.; Yang, Y.-F.; Su, A. Transfer Learning across Different Chemical Domains: Virtual Screening of Organic Materials with Deep Learning Models Pretrained on Small Molecule and Chemical Reaction Data. *J. Cheminform.* **2024**, *16*, 89. [CrossRef]
46. Zheng, X.; Lin, L.; Liu, B.; Xiao, Y.; Xiong, X. A Multi-Task Transfer Learning Method with Dictionary Learning. *Knowl.-Based Syst.* **2020**, *191*, 105233. [CrossRef]
47. Fan, X.; Gong, M.; Tang, Z.; Wu, Y. Deep Neural Message Passing With Hierarchical Layer Aggregation and Neighbor Normalization. *IEEE Trans. Neural Netw. Learn. Syst.* **2022**, *33*, 7172–7184. [CrossRef]
48. Tingle, B.I.; Tang, K.G.; Castanon, M.; Gutierrez, J.J.; Khurelbaatar, M.; Dandarchuluun, C.; Moroz, Y.S.; Irwin, J.J. ZINC-22–A Free Multi-Billion-Scale Database of Tangible Compounds for Ligand Discovery. *J. Chem. Inf. Model.* **2023**, *63*, 1166–1176. [CrossRef]
49. Wang, X.; Li, Y.; Qiu, J.; Chen, G.; Liu, H.; Liao, B.; Hsieh, C.-Y.; Yao, X. RetroPrime: A Diverse, Plausible and Transformer-Based Method for Single-Step Retrosynthesis Predictions. *Chem. Eng. J.* **2021**, *420*, 129845. [CrossRef]
50. Kovács, D.P.; McCorkindale, W.; Lee, A.A. Quantitative Interpretation Explains Machine Learning Models for Chemical Reaction Prediction and Uncovers Bias. *Nat. Commun.* **2021**, *12*, 1695. [CrossRef]
51. Yang, X.; Wang, H.; Zhang, Y.; Su, W.; Yu, J. Generation of Aryl Radicals from in Situ Activated Homolytic Scission: Driving Radical Reactions by Ball Milling. *Green Chem.* **2022**, *24*, 4557–4565. [CrossRef]
52. Liu, L.; Ward, R.M.; Schomaker, J.M. Mechanistic Aspects and Synthetic Applications of Radical Additions to Allenes. *Chem. Rev.* **2019**, *119*, 12422–12490. [CrossRef] [PubMed]
53. Jabor Gozzi, G.; Bouaziz, Z.; Winter, E.; Daflon-Yunes, N.; Aichele, D.; Nacereddine, A.; Marminon, C.; Valdameri, G.; Zeinyeh, W.; Bollacke, A.; et al. Converting Potent Indeno[1,2-b]Indole Inhibitors of Protein Kinase CK2 into Selective Inhibitors of the Breast Cancer Resistance Protein ABCG2. *J. Med. Chem.* **2015**, *58*, 265–277. [CrossRef] [PubMed]
54. Mondal, S.; Mohamed, R.K.; Manoharan, M.; Phan, H.; Alabugin, I.V. Drawing from a Pool of Radicals for the Design of Selective Enyne Cyclizations. *Org. Lett.* **2013**, *15*, 5650–5653. [CrossRef]
55. Takase, M.; Narita, T.; Fujita, W.; Asano, M.S.; Nishinaga, T.; Benten, H.; Yoza, K.; Müllen, K. Pyrrole-Fused Azacoronene Family: The Influence of Replacement with Dialkoxybenzenes on the Optical and Electronic Properties in Neutral and Oxidized States. *J. Am. Chem. Soc.* **2013**, *135*, 8031–8040. [CrossRef] [PubMed]
56. Hou, Z.-W.; Mao, Z.-Y.; Song, J.; Xu, H.-C. Electrochemical Synthesis of Polycyclic N-Heteroaromatics through Cascade Radical Cyclization of Diynes. *ACS Catal.* **2017**, *7*, 5810–5813. [CrossRef]
57. Monfette, S.; Turner, Z.R.; Semproni, S.P.; Chirik, P.J. Enantiopure C1-Symmetric Bis(Imino)Pyridine Cobalt Complexes for Asymmetric Alkene Hydrogenation. *J. Am. Chem. Soc.* **2012**, *134*, 4561–4564. [CrossRef]
58. Zhang, S.; Bedi, D.; Cheng, L.; Unruh, D.K.; Li, G.; Findlater, M. Cobalt(II)-Catalyzed Stereoselective Olefin Isomerization: Facile Access to Acyclic Trisubstituted Alkenes. *J. Am. Chem. Soc.* **2020**, *142*, 8910–8917. [CrossRef]
59. Wang, Q.; Yang, X.; Wu, P.; Yu, Z. Photoredox-Catalyzed C–H Arylation of Internal Alkenes to Tetrasubstituted Alkenes: Synthesis of Tamoxifen. *Org. Lett.* **2017**, *19*, 6248–6251. [CrossRef]
60. Alizadeh, S.R.; Ebrahimzadeh, M.A. O-Glycoside Quercetin Derivatives: Biological Activities, Mechanisms of Action, and Structure–Activity Relationship for Drug Design, a Review. *Phytother. Res.* **2022**, *36*, 778–807. [CrossRef]
61. Noguchi, H.; Hojo, K.; Suginome, M. Boron-Masking Strategy for the Selective Synthesis of Oligoarenes via Iterative Suzuki−Miyaura Coupling. *J. Am. Chem. Soc.* **2007**, *129*, 758–759. [CrossRef]
62. Lo, J.C.; Gui, J.; Yabe, Y.; Pan, C.-M.; Baran, P.S. Functionalized Olefin Cross-Coupling to Construct Carbon–Carbon Bonds. *Nature* **2014**, *516*, 343–348. [CrossRef]

Disclaimer/Publisher's Note: The statements, opinions and data contained in all publications are solely those of the individual author(s) and contributor(s) and not of MDPI and/or the editor(s). MDPI and/or the editor(s) disclaim responsibility for any injury to people or property resulting from any ideas, methods, instructions or products referred to in the content.